Multifunctional Organic Materials

DOI: 10.1002/anie.201205439

A Multifunctional Porous Organic Schottky Barrier Diode**

*Sasanka Dalapati, Rajat Saha, Sankar Jana, Astam K. Patra, Asim Bhaumik, Sanjay Kumar, and Nikhil Guchhait**

For the past two decades scientists have been engaged in designing and synthesizing porous metal–organic frameworks (MOFs) capable for gas and solvent adsorption.[1,2] From the middle of the last decade, researchers have tried to include many functional properties in a single framework. Thus multifunctional MOFs[3–5] were developed as materials with a set of well-defined properties, for example, porosity and magnetism, porosity and electrical conductivity, or porosity and optical properties. This synergism, resulting from the combination of two different functionalities, opens up the way to new multifunctional materials.

In the last two years, a large number of porous covalent organic frameworks were reported by different research groups worldwide and they have shown that in porous organic materials (POMs) a degree of porosity can be achieved which is higher than in MOFs.[6–8] In the case of 3D MOFs, several modifications are needed to achieve higher porosity, such as generation of unsaturated metal centers (UMCs) and formation of hydrophobic channels. In contrast to 3D MOFs, adsorption by supramolecular 3D POMs occurs in several steps because of their structural flexibility.[8–10] Regarding materials with a similar degree of porosity, the molecular weight of POMs is lower than that of MOFs and zeolites. Thus, it can be said that the adsorption properties of porous organic materials (POMs) are better than those of other porous materials like MOFs and zeolites because of their high flexibility, multistep adsorption process, and low molecular weight.

Recently, some research groups were engaged in establishing multifunctional properties in POMs.[11–15] Here, we also synthesized a multifunctional porous organic material, 2,6-bis-(2-amino-5-nitro-phenyl)-pyrrolo[3,4-f]isoindole-1,3,5,7-tetraone (ANPPIT, see the Supporting Information), and characterized this material by single-crystal X-ray diffraction analysis, NMR and IR spectroscopy, PXRD, and thermal studies. This material is porous after removal of the dimethylformamide (DMF) and the water guest molecules. The porosity of this material has been studied by N_2 adsorption at 77 K. Further, to show the multifunctional character of the material, we have studied its *I-V* characteristic and guest-dependent luminescence property.

Slow Et_2O vapor diffusion in DMF solution of ANPPIT affords yellow rhombic crystal suitable for X-ray diffraction at room temperature (see the Supporting Information).[16] The diffraction analysis indicates that the compound crystallizes in an achiral *C*2/*c* space group (see Table S1 in the Supporting Information). Each asymmetric unit contains half of the ANPPIT moiety with one DMF and 1.5 water guest molecules. Within the molecular structure, *p*-nitroaniline (PNA) units are nearly perpendicular to the basic pyrrolo[3,4-f]isoindole-1,3,5,7-tetraone moiety (Figure 1), that forms

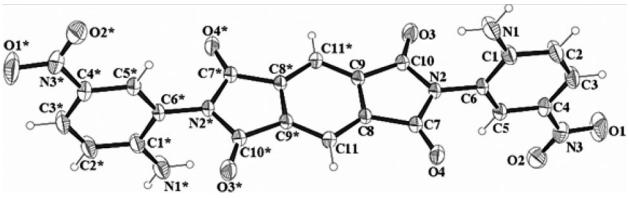

Figure 1. ORTEP view of ANPPIT without guest molecules (DMF and water) at a 30% probability.

a 3D architecture by H-bonding and π interactions (Figures S1, S2 and Tables S2, S3 in the Supporting Information). Each molecular unit is connected to four other units through N1–H2···O4 hydrogen-bonding interactions and thus a 3D supramolecular architecture is formed (Figure S1). During the packing process, a 1D channel is generated along the crystallographic *c* axis (Figure 2). The diameter of the channel is 17.3×7.0 Å^2. Water and DMF guest molecules persist within the channels through supramolecular hydrogen-bonding interactions (Figure S3). The guest water molecules are connected by hydrogen-bonding interactions leading to the formation of a 1D helical chain (Figure S4).

Thermal analysis reveals that at 120 °C all DMF and water guest molecules are removed and the evacuated framework is stable up to 230 °C without any further loss of weight (Figure S5). The powder X-ray diffraction (PXRD) pattern, obtained after removal of the guest molecules by heating at 120 °C for 3 h, indicates that the evacuated framework remains crystalline (Figure S6). However, there is a change in the PXRD patterns of different materials which leads to the conclusion that a structural transformation occurs upon removal of the guest molecules followed by the formation

[*] S. Dalapati, S. Jana, Dr. N. Guchhait
Department of Chemistry, University of Calcutta
92 A.P.C. Road, Kolkata (India)
E-mail: nguchhait@yahoo.com
R. Saha, Dr. S. Kumar
Department of Physics, Jadavpur University, Kolkata (India)
A. K. Patra, Dr. A. Bhaumik
Department of Materials Science, Indian Association for the Cultivation of Science, Kolkata (India)

[**] N.G. acknowledges the DST (project number SR/S1/PC/26/2008). S.D. and S.J. acknowledge UGC for a fellowship. A.K.P. and R.S. is thankful to the CSIR, New Delhi. We thank S.K.'s colleague, Dr. P. P. Ray, for valuable discussion.

Supporting information for this article is available on the WWW under http://dx.doi.org/10.1002/anie.201205439.

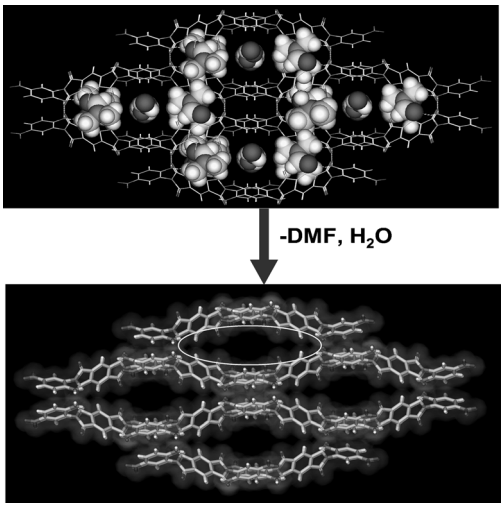

Figure 2. 3D supramolecular structure with a 1D channel along the *c* axis (DMF and water guest molecules persist within the channels).

of a new framework with a diffraction peak at 7.16° for 2θ. PLATON[17] analysis suggests that the compound contains a potential solvent-accessible void space of 1583.3 Å^3 (46.2%, Figure 2). The high stability and flexibility of the supramolecular framework after loss of the guest molecules allows us to study the adsorption behavior of ANPPIT.

The N_2 adsorption study has been carried out with the evacuated framework at 77 K (see the Supporting Information). Following the general classification of adsorption isotherms, the adsorption profile can be classified as type II (Figure 3). The Brunauer–Emmett–Teller (BET) surface area and the respective pore volume have been determined to be 93.2 $m^2 g^{-1}$ and 0.21 $cc\,g^{-1}$, respectively. The pore size distribution of the sample using the NLDFT model (N_2 adsorption on carbon as reference) suggested that ANPPIT has an average pore width of about 4.9 nm, which could be attributed to interparticle mesopores. The isotherm shows that at a low pressure (P/P_0 of about 0) the material adsorbs a certain amount of gas (about 5 mL), which could be attributed to

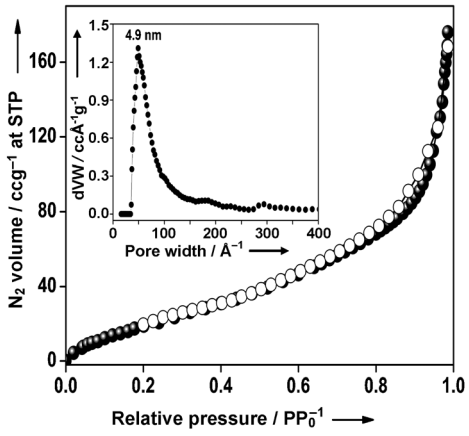

Figure 3. N_2 adsorption (●)–desorption (○) isotherm at 77 K (inset, the pore size distribution of the sample calculated using the NLDFT model). STP = standard temperature and pressure.

monolayer adsorption at the void surfaces. However, at higher pressure (in the P/P_0 range of 0.01–0.80) the quantity of adsorbed gas increases monotonically. After $P/P_0 = 0.80$, the quantity of adsorbed gas (178 mL) sharply increases without saturation at $P/P_0 = 1$.

This adsorption phenomenon can be explained through the occurrence of "stepwise adsorption". Stepwise adsorption has been observed for 3D supramolecular MOFs which are hosting the adsorbate molecules in their framework.[5a,18] The supramolecular interactions induce flexibility within the framework. Up to a certain pressure, adsorbate molecules cannot enter into the void spaces but when a certain pressure is reached, the pores are open and at this pressure a large amount of adsorbate molecules enters into the void spaces. Supramolecular interactions are rather weak forces. The discrete units packed by supramolecular interactions can be moved by the external pressure and thus a "gate-opening" process is observed.[8] For POMs, which show extrinsic porosity, the discrete molecules/building blocks are packed through supramolecular interactions. Thus, POMs with "framework flexibility" are mostly associated with "stepwise adsorption".[8] In the present case, there is a stiff increase in the adsorption of N_2 from 70 mL at $P/P_0 = 0.80$ to 178 mL at $P/P_0 = 1$. Thus, it can be said that after $P/P_0 = 0.8$ this supramolecular and flexible framework undergoes structural transformation to achieve a higher porosity which may be indicative of "gate opening".

To show a guest-dependent optical property, we have studied the luminescence behavior of the synthesized compound (ANPPIT with 3 H_2O and 2 DMF guest molecules) and the evacuated framework in the solid state. Both compounds exhibit similar absorption behavior with bands at about 315 and 390 nm (Figure S7), which corresponds to the π–π* transition of the benzene chromophore and the intermolecularly conjugated π-stacked framework, respectively.[19,20a] The guest-filled compound shows an extra broad band at about 500 nm, which can be attributed to charge transfer from the electron-rich NH_2 to the electron-withdrawing NO_2 group or in the pyrrolo[3,4-f]isoindole-1,3,5,7-tetraone moiety in the presence of polar guest molecules (DMF and H_2O). Upon excitation at 390 nm, the compound (ANPPIT with 3 H_2O and 2 DMF guest molecules) shows well-separated emission bands at about 450, 480, and 525 nm (Figure 4a). These bands correspond to different π-electronic transition in the packed molecular system.[19] Upon removal of guest molecules, a remarkable emission enhancement was observed by keeping the highly structured bands unaltered. Fluorescence enhancement can be attributed to the inhibition of energy transfer (nonradiative decay) through polar guest molecules. However, both compounds (ANPPIT with and without guest molecules) exhibit similar but less intense luminescence spectra (Figure S8) upon excitation at 315 nm.

Recently, extended π-conjugated organic supramolecular compounds have emerged as promising semiconducting materials.[19] These organic semiconducting materials are generally used for the fabrication of several electronic devices such as field effect transistors (FETs), light-emitting diodes (LEDs), photovoltaic cells (PCs), and Schottky barrier diodes.[20–22] Metal–semiconductor rectifying contacts are

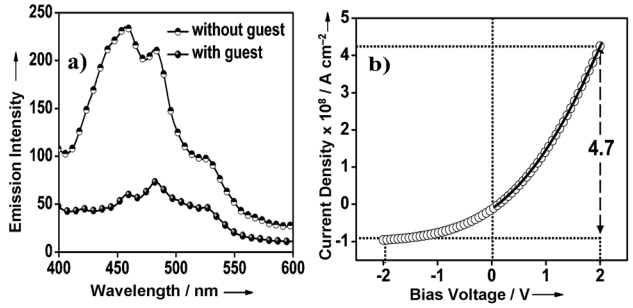

Figure 4. a) Guest-dependent photoluminescence (λ_{ex} = 390 nm) and b) *I-V* characteristics of ANPPIT at room temperature. *I-V* curve: a solid black line indicates the fitting curve at a forward bias voltage and 4.7 is the $I(2\,V)/I(-2\,V)$ ratio.

generally referred to as "Schottky barrier diode".[22,23] Organic Schottky barrier diodes are undoubtedly the "key active element" of the next generation of semiconducting devices. The current–voltage (*I-V*) characteristic (Figure 4b and Figure S9) for the "ITO/sample/Al" sandwich structure (ITO = indium–tin oxide and sample = ANPPIT) and a curve fitted to the simplest diode equation[23] are shown in Figure 4b (fitting has been carried out in forward bias voltage only). The *I-V* curve of the junction exhibits a nonlinear behavior and shows rectifying properties. The rectification ratio $I(2\,V)/I(-2\,V)$ is 4.7. The semiconducting properties of the material (ANPPIT) most likely originate from the extended π-conjugated electrons (a π-stacking distance of 3.816 Å in Figure S2). The experimental band gap (E_{opt} = 2.88 eV, Figure S10) shows reasonable agreement with theoretical[20b] results (E_{theo} = 2.87 eV, Figure S11), which suggests that the relatively low-lying LUMO (E_{LUMO} = −3.98 eV, see the Supporting Information) level is responsible for carrier conduction (LUMO = lowest unoccupied molecular orbital).[20c] Thus, "ANPPIT-Al" and "ANPPIT-ITO" junctions are working as Ohmic contact and Schottky barrier diode, respectively or vice versa, owing to their work functions (Al: 4.3 eV and ITO: 4.7 eV).[23b]

In summary, we have successfully designed and synthesized a purely organic porous material {2,6-bis-(2-amino-5-nitro-phenyl)-pyrrolo[3,4-f]isoindole-1,3,5,7-tetraone, ANPPIT} of relatively low molecular weight. The single-crystal X-ray diffraction analysis shows that its 3D architecture is formed through H-bonding and π interactions which undoubtedly characterize its porosity, guest-dependent luminescence, and electrical properties. This may be useful for the future construction of multifunctional materials with low molecular weight. The discovery of multifunctional materials obtained by a simple low-cost method is a breakthrough in an area of current chemical interest.

Received: July 10, 2012
Revised: September 29, 2012
Published online: November 5, 2012

Keywords: adsorption · electrical conductivity · luminescence · mesoporous materials · X-ray diffraction

[1] O. M. Yaghi, M. O'Keeffe, N. W. Ockwig, H. K. Chae, M. Eddaoudi, J. Kim, *Nature* **2003**, *423*, 705–714.
[2] a) R. Matsuda, R. Kitaura, S. Kitagawa, Y. Kubota, T. C. Kobayashi, S. Horike, M. Takata, *J. Am. Chem. Soc.* **2004**, *126*, 14063–14070; b) H. Deng, S. Grunder, K. E. Cordova, C. Valente, H. Furukawa, M. Hmadeh, F. Gándara, A. C. Whalley, Z. Liu, S. Asahina, H. Kazumori, M. O'Keeffe, Ó. Terasaki, J. F. Stoddart, O. M. Yaghi, *Science* **2012**, *336*, 1018–1023; c) M. Higuchi, K. Nakamura, S. Horike, Y. Hijikata, N. Yanai, T. Fukushima, J. Kim, K. Kato, M. Takata, D. Watanabe, S. Oshima, S. Kitagawa, *Angew. Chem.* **2012**, *124*, 8494–8497; *Angew. Chem. Int. Ed.* **2012**, *51*, 8369–8372.
[3] S. Kitagawa, R. Kitaura, S.-I. Noro, *Angew. Chem.* **2004**, *116*, 2388–2430; *Angew. Chem. Int. Ed.* **2004**, *43*, 2334–2375.
[4] R. J. Kuppler, D. J. Timmons, Q.-R. Fang, J.-R. Li, T. A. Makal, M. D. Young, D. Yuan, D. Zhao, W. Zhuang, H.-C. Zhou, *Coord. Chem. Rev.* **2009**, *253*, 3042–3066.
[5] a) X. Ding, J. Guo, X. Feng, Y. Honsho, J. Guo, S. Seki, P. Maitarad, A. Saeki, S. Nagase, D. Jiang, *Angew. Chem.* **2011**, *123*, 1325–1329; *Angew. Chem. Int. Ed.* **2011**, *50*, 1289–1293; b) S. Kitagawa, R. Kitaura, S.-I. Noro, *Angew. Chem.* **2004**, *116*, 2388–2430; *Angew. Chem. Int. Ed.* **2004**, *43*, 2334–2375; c) R. Saha, S. Kumar, *CrystEngComm* **2012**, *14*, 4980–4988.
[6] a) T. Hasell, S. Y. Chong, K. E. Jelfs, D. J. Adams, A. I. Cooper, *J. Am. Chem. Soc.* **2012**, *134*, 588–598; b) M. Rose, W. Böhlmann, M. Sabo, S. Kaskel, *Chem. Commun.* **2008**, 2462–2464.
[7] a) W. Yang, A. Greenaway, X. Lin, R. Matsuda, A. J. Blake, C. Wilson, W. Lewis, P. Hubberstey, S. Kitagawa, N. R. Champness, M. Schröder, *J. Am. Chem. Soc.* **2010**, *132*, 14457–14469; b) S. Lim, H. Kim, N. Selvapalam, K.-J. Kim, S. J. Cho, G. Seo, K. Kim, *Angew. Chem.* **2008**, *120*, 3400–3403; *Angew. Chem. Int. Ed.* **2008**, *47*, 3352–3355.
[8] a) M. Mastalerz, I. M. Oppel, *Angew. Chem.* **2012**, *124*, 5345–5348; *Angew. Chem. Int. Ed.* **2012**, *51*, 5252–5255; b) T. Mitra, X. Wu, R. Clowes, J. T. A. Jones, K. E. Jelfs, D. J. Adams, A. Trewin, J. Bacsa, A. Steiner, A. I. Cooper, *Chem. Eur. J.* **2011**, *17*, 10235–10240.
[9] A. P. Côté, H. M. El-Kaderi, H. Furukawa, J. R. Hunt, O. M. Yaghi, *J. Am. Chem. Soc.* **2007**, *129*, 12914–12915.
[10] J. Tian, P. K. Thallapally, B. P. McGrail, *CrystEngComm* **2012**, *14*, 1909–1919.
[11] S. Wan, F. Gándara, A. Asano, H. Furukawa, A. Saeki, S. K. Dey, L. Liao, M. W. Ambrogio, Y. Y. Botros, X. Duan, S. Seki, J. F. Stoddart, O. M. Yaghi, *Chem. Mater.* **2011**, *23*, 4094–4097.
[12] X. Ding, L. Chen, Y. Honsho, X. Feng, O. Saengsawang, J. Guo, A. Saeki, S. Seki, S. Irle, S. Nagase, V. Parasuk, D. Jiang, *J. Am. Chem. Soc.* **2011**, *133*, 14510–14513.
[13] a) S. Wan, J. Guo, J. Kim, H. Ihee, D. Jiang, *Angew. Chem.* **2008**, *120*, 8958–8962; *Angew. Chem. Int. Ed.* **2008**, *47*, 8826–8830; b) A. Popp, J. J. Schneider, *Angew. Chem.* **2008**, *120*, 9092–9095; *Angew. Chem. Int. Ed.* **2008**, *47*, 8958–8962.
[14] a) X. Feng, L. Liu, Y. Honsho, A. Saeki, S. Seki, S. Irle, Y. Dong, A. Nagai, D. Jiang, *Angew. Chem.* **2012**, *124*, 2672–2676; *Angew. Chem. Int. Ed.* **2012**, *51*, 2618–2622; b) D. Chandra, B. K. Jena, C. R. Raj, A. Bhaumik, *Chem. Mater.* **2007**, *19*, 6290–6296.
[15] M. Yoon, K. Suh, H. Kim, Y. Kim, N. Selvapalam, K. Kim, *Angew. Chem.* **2011**, *123*, 8016–8019; *Angew. Chem. Int. Ed.* **2011**, *50*, 7870–7873.
[16] CCDC 886757 (ANPPIT) contains the supplementary crystallographic data for this paper. These data can be obtained free of charge from The Cambridge Crystallographic Data Centre via www.ccdc.cam.ac.uk/data_request/cif.
[17] PLATON, Molecular Geometry Program: A. L. Spek, *J. Appl. Crystallogr.* **2003**, *36*, 7.

[18] R. Kitaura, K. Seki, G. Akiyama, S. Kitagawa, *Angew. Chem.* **2003**, *115*, 444 – 447; *Angew. Chem. Int. Ed.* **2003**, *42*, 428 – 431.
[19] a) Y. Cui, H. Xu, Y. Yue, Z. Guo, J. Yu, Z. Chen, J. Gao, Y. Yang, G. Qian, B. Chen, *J. Am. Chem. Soc.* **2012**, *134*, 3979 – 3982; b) D. F. Sava, L. E. S. Rohwer, M. A. Rodriguez, T. M. Nenoff, *J. Am. Chem. Soc.* **2012**, *134*, 3983 – 3986.
[20] a) A.-D. Yu, T. Kurosawa, Y.-C. Lai, T. Higashihara, M. Ueda, C.-L. Liu, W.-C. Chen, *J. Mater. Chem.* **2012**, DOI: 10.1039/c2m33852a; b) L. Chen, L. Wang, X. Gao, S. Nagase, Y. Honsho, A. Saeki, S. Seki, D. Jiang, *Chem. Commun.* **2009**, 3119 – 3121; c) M. Huang, U. Schilde, M. Kumke, M. Antonietti, H. Cölfen, *J. Am. Chem. Soc.* **2010**, *132*, 3700 – 3707; d) Q. Zheng, J. Huang, A. Sarjeant, H. E. Katz, *J. Am. Chem. Soc.* **2008**, *130*, 14410 – 14411.
[21] a) K. Niimi, H. Mori, E. Miyazaki, I. Osaka, H. Kakizoe, K. Takimiya, C. Adachi, *Chem. Commun.* **2012**, *48*, 5892 – 5894; b) S.-C. Chen, Q. Zhang, Q. Zheng, C. Tang, C.-Z. Lu, *Chem. Commun.* **2012**, *48*, 1254 – 1256.
[22] M. L. Chabinyc, X. Chen, R. E. Holmlin, H. Jacobs, H. Skulason, C. D. Frisbie, V. Mujica, M. A. Ratner, M. A. Rampi, G. M. Whitesides, *J. Am. Chem. Soc.* **2002**, *124*, 11730 – 11736.
[23] a) R. K. Gupta, R. A. Singh, *J. Mater. Sci. Mater. Electron.* **2005**, *16*, 253 – 256; b) T. Kaji, T. Takenobu, A. F. Morpurgo, Y. Iwasa, *Adv. Mater.* **2009**, *21*, 3689 – 3693; c) Ş. Aydoğan, Ö. Güllü, A. Türüt, *Phys. Scr.* **2009**, *79*, 035802.
[24] B. G. Streetman, *Solid state electronic devices*, 4th ed., Prentice hall of India, **2000**, pp. 184 – 190.

